

advances.sciencemag.org/cgi/content/full/6/26/eaba3139/DC1

Supplementary Materials for

Single yeast cell nanomotions correlate with cellular activity

Ronnie G. Willaert*, Pieterjan Vanden Boer, Anton Malovichko, Mitchel Alioscha-Perez, Ksenija Radotić, Dragana Bartolić, Aleksandar Kalauzi, Maria Ines Villalba, Dominique Sanglard, Giovanni Dietler, Hichem Sahli, Sandor Kasas*

*Corresponding author. Email: ronnie.willaert@vub.be (R.G.W.); sandor.kasas@epfl.ch (S.K.)

Published 24 June 2020, *Sci. Adv.* **6**, eaba3139 (2020)
DOI: 10.1126/sciadv.aba3139

The PDF file includes:

Figs. S1 to S9
Table S1
Legends for movies S1 to S4
References

Other Supplementary Material for this manuscript includes the following:

(available at advances.sciencemag.org/cgi/content/full/6/26/eaba3139/DC1)

Movies S1 to S4

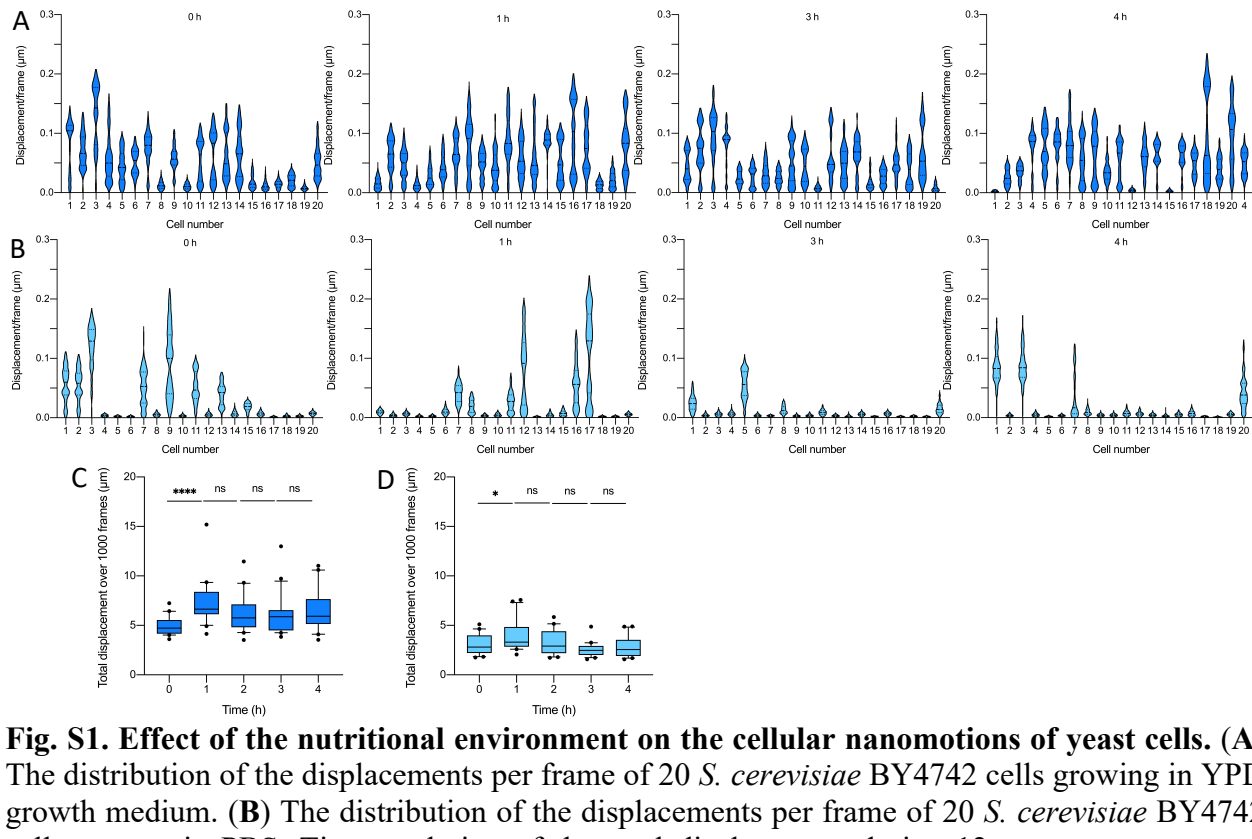


Fig. S1. Effect of the nutritional environment on the cellular nanomotions of yeast cells. (A) The distribution of the displacements per frame of 20 *S. cerevisiae* BY4742 cells growing in YPD growth medium. (B) The distribution of the displacements per frame of 20 *S. cerevisiae* BY4742 cells present in PBS. Time evolution of the total displacement during 12 s measurement as a function of time for cells (C) in YPD growth medium, and (D) in PBS. Wilcoxon test: **** P < 0.0001; * P < 0.1; ns: not significant.

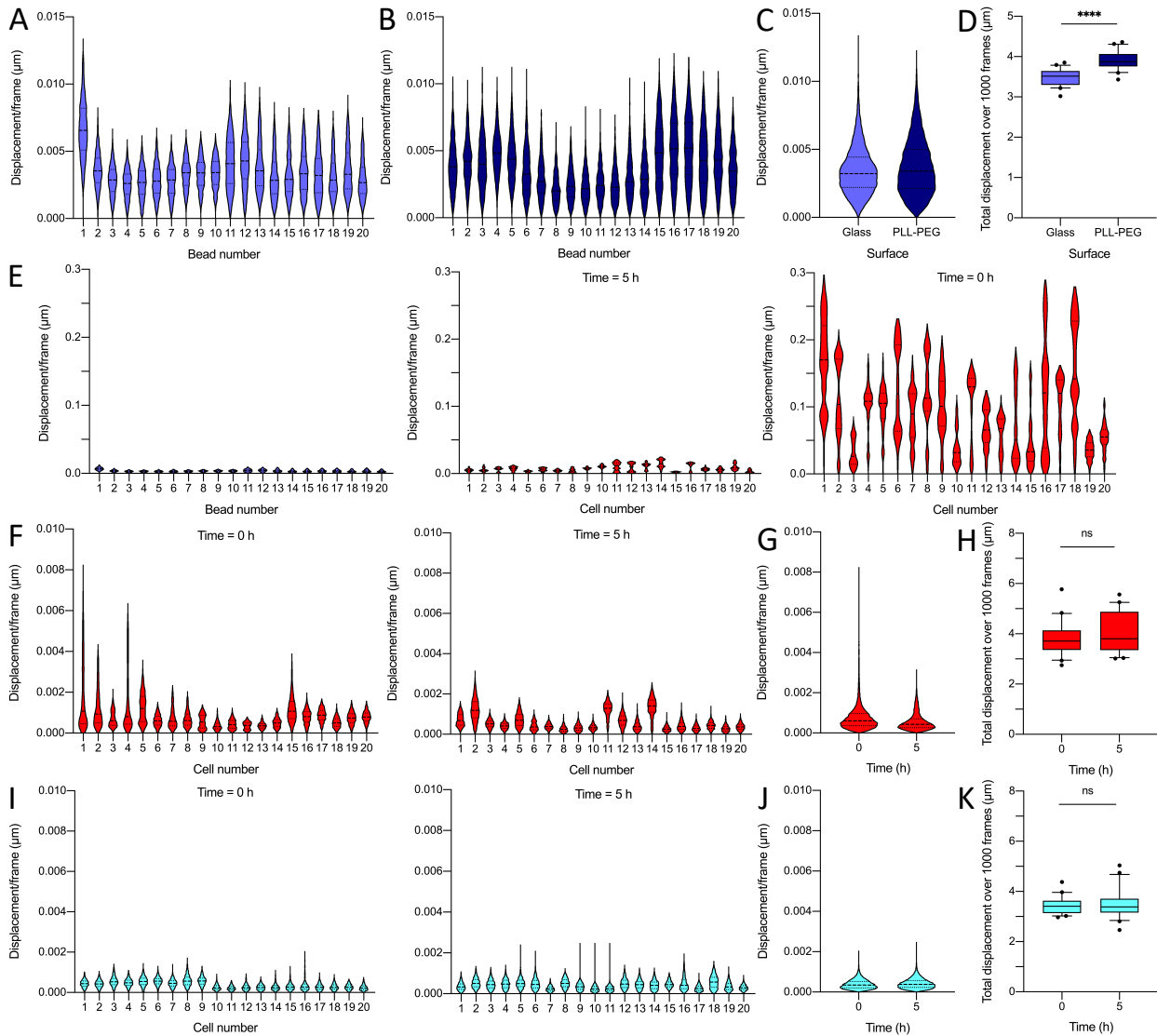


Fig. S2. Movements of silica microbeads and adhesion of cells to the glass surface by concanavalin A. **A.** The displacement/frame for 20 beads on (A) a glass surface and (B) PLL-PEG treated surface. (C) Displacements per frame of all 20 beads on a glass and PLL-PEG treated surface. (D) The total displacement during 12 s measurement of beads on a glass and PLL-PEG treated surface. Wilcoxon test: **** P < 0.0001. (E) Comparison of the displacement/frame for 20 beads on glass (left panel) to amphotericin (500 μg/ml) treated (center panel) *C. albicans* DSY294 and untreated cells (right panel). The displacement/frame of 20 cells untreated (left panel) and caspofungin (10 μg/ml) treated cells after 5 h (right panel) for (F) the wild-type *C. albicans* DSY294 and (I) the hypersusceptible *C. albicans* DSY1024 strain. Displacements per frame of all 20 (G) *C. albicans* DSY294 and (J) *C. albicans* DSY1024 cells. The total displacement during 12 s measurement of 20 (H) *C. albicans* DSY294 and (K) *C. albicans* DSY1024 cells.

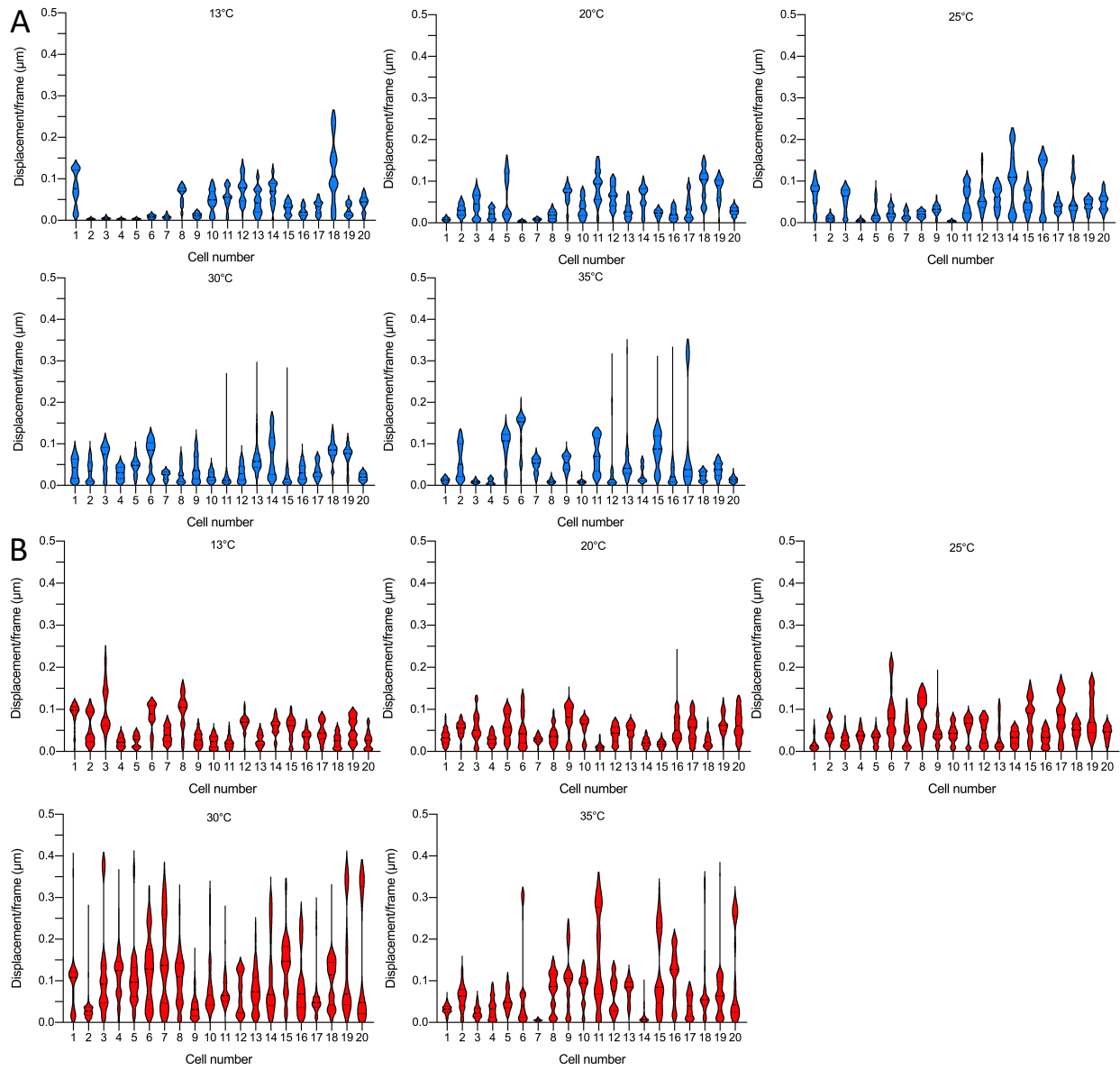


Fig. S3. Effect of the temperature on the cellular nanomotions of yeast cells. The distribution of the displacements per frame of 20 cells as function of the temperature (13°C, 20°C, 25°C, 30°C, 35°C) for (A) *S. cerevisiae* BY4742 and (B) *C. albicans* DSY294.

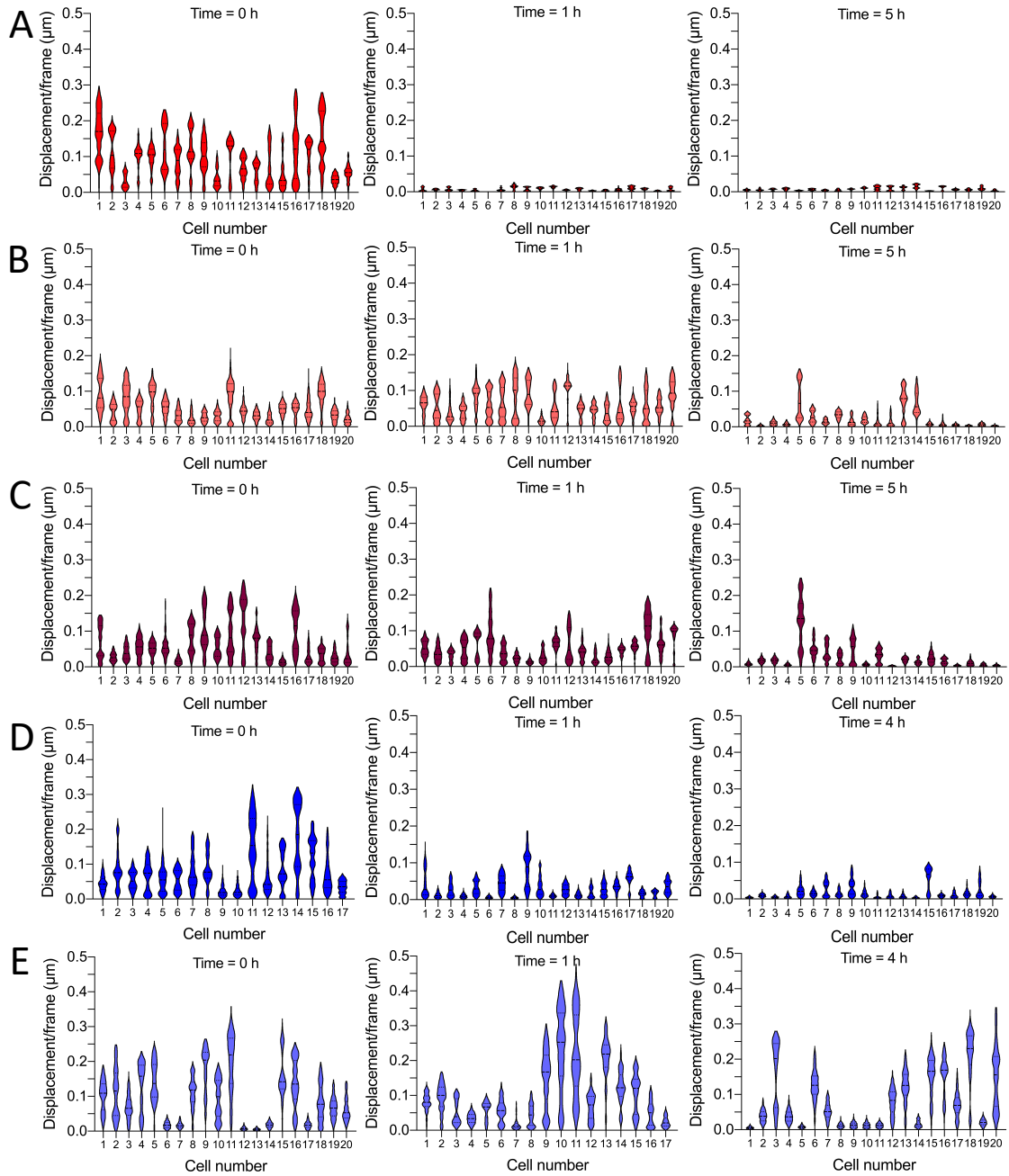


Fig. S4. Effect of antifungals on the cellular nanomotion of *C. albicans*. The displacement/frame of 20 *C. albicans* DSY294 cells treated with (A) amphotericin B (500 $\mu\text{g}/\text{ml}$), (B) caspofungin (100 $\mu\text{g}/\text{ml}$), and (C) fluconazole (400 $\mu\text{g}/\text{ml}$). The displacement/frame of 20 (D) hypersusceptible *C. albicans* DSY1024 cells and (E) the candin-resistant *C. albicans* DSY4614 cells treated with caspofungin (10 $\mu\text{g}/\text{ml}$).

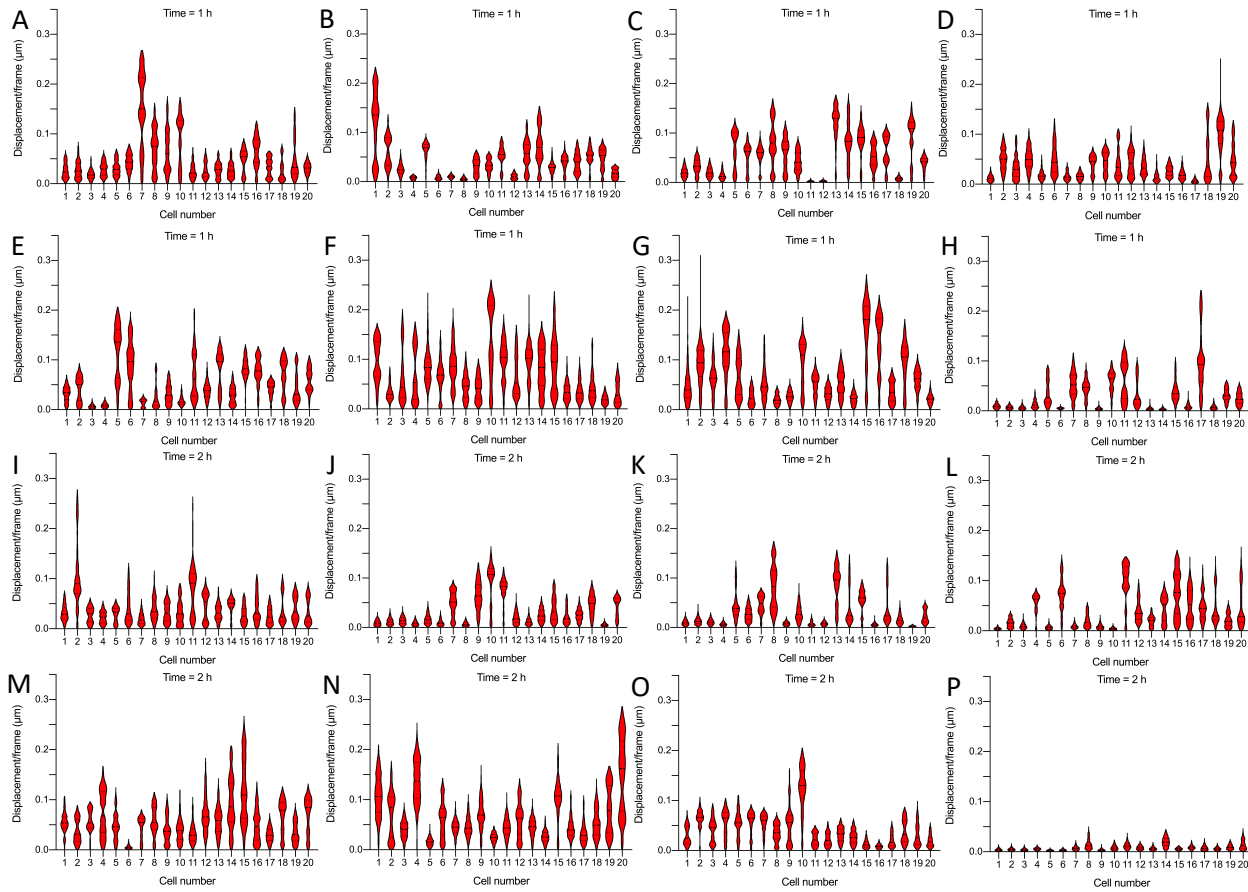


Fig. S5. Effect of increasing amphotericin B concentrations on *C. albicans* DSY294 wild-type strain. Cellular displacements per frame after 1 h for (A) untreated cells, (B) $0.1 \mu\text{g/ml}$, (C) $0.5 \mu\text{g/ml}$, (D) $1 \mu\text{g/ml}$, (E) $4 \mu\text{g/ml}$, (F) $10 \mu\text{g/ml}$, (G) $50 \mu\text{g/ml}$, (H) $100 \mu\text{g/ml}$. Cellular displacements per frame after 2 h for (I) untreated cells, (J) $0.1 \mu\text{g/ml}$, (K) $0.5 \mu\text{g/ml}$, (L) $1 \mu\text{g/ml}$, (M) $4 \mu\text{g/ml}$, (N) $10 \mu\text{g/ml}$, (O) $50 \mu\text{g/ml}$, (P) $100 \mu\text{g/ml}$.

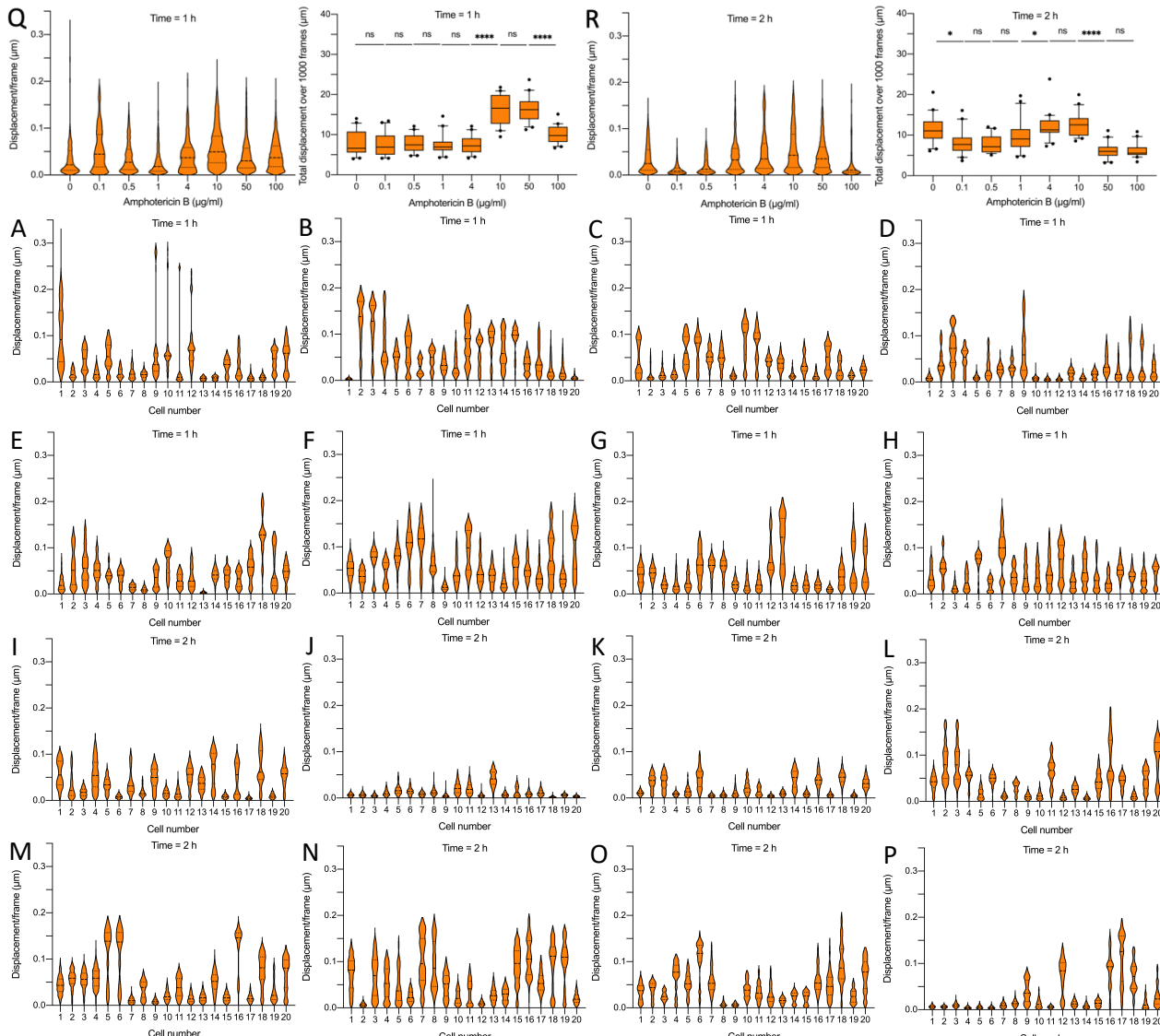


Fig. S6. Effect of increasing amphotericin B concentrations on *C. albicans* CAF2-1 wild-type strain. Cellular displacements per frame after 1 h for (A) untreated cells, (B) 0.1 µg/ml, (C) 0.5 µg/ml, (D) 1 µg/ml, (E) 4 µg/ml, (F) 10 µg/ml, (G) 50 µg/ml, (H) 100 µg/ml. Cellular displacements per frame after 2 h for (I) untreated cells, (J) 0.1 µg/ml, (K) 0.5 µg/ml, (L) 1 µg/ml, (M) 4 µg/ml, (N) 10 µg/ml, (O) 50 µg/ml, (P) 100 µg/ml. (Q) Cellular displacements per frame (left panel) and the total displacement per frame for 20 cells (right panel) after 1 h treatment, and (R) after 2 h treatment. Wilcoxon test: **** P < 0.0001; * P < 0.1; ns: not significant.

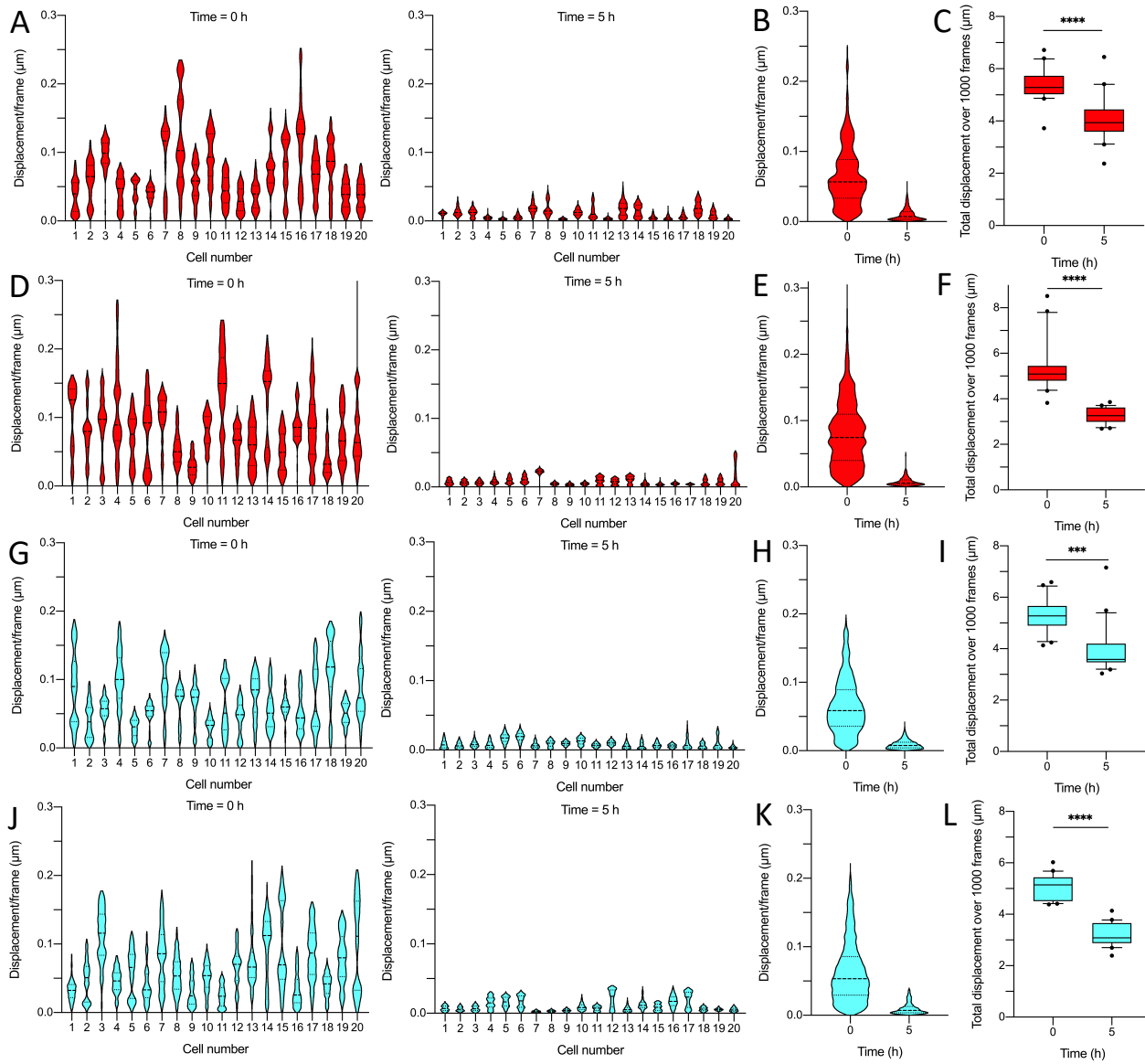


Fig. S7. Effect of the surface on cellular movement of *C. albicans*. The displacement/frame of 20 *C. albicans* DSY294 cells untreated (left panel) and caspofungin (10 $\mu\text{g}/\text{ml}$) treated cells (right panel) on (A) a PLL-PEG treated and (D) glass surface. Displacements per frame of all 20 cells on (B) a PLL-PEG and (E) a glass treated surface. The total displacement during 12 s measurement of 20 cells on (C) a PLL-PEG and (F) glass treated surface. The displacement/frame of 20 *C. albicans* DSY1024 cells untreated (left panel) and caspofungin (10 $\mu\text{g}/\text{ml}$) treated cells (right panel) on (G) a PLL-PEG treated and (J) glass surface. Displacements per frame of all 20 cells on (H) a PLL-PEG and (K) a glass treated surface. The total displacement during 12 s measurement of 20 cells on (I) a PLL-PEG and (L) glass treated surface. Wilcoxon test: **** $P < 0.0001$, *** $P < 0.001$.

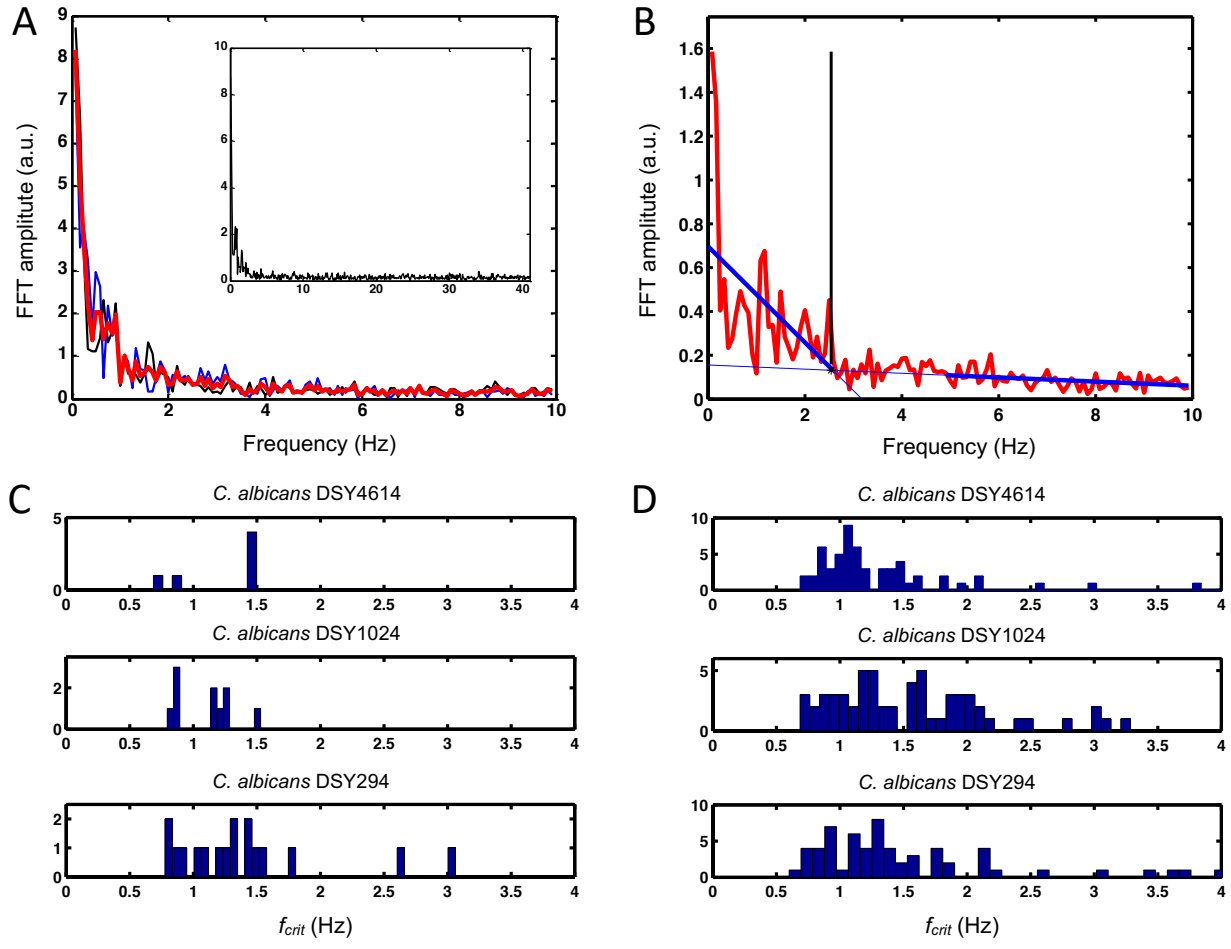
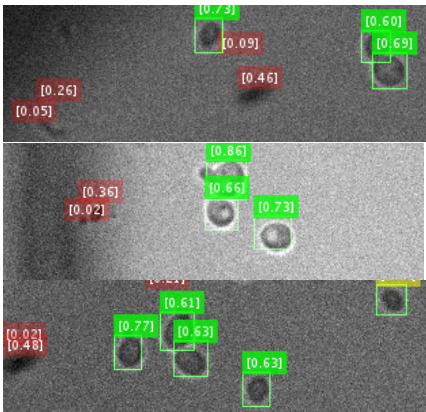
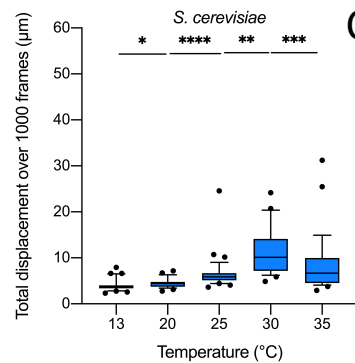


Fig. S8. Determination of the frequency range of cell movements and critical frequency. (A) Typical FFT spectra obtained from two optically recorded signals of one *C. albicans* cell movements in the horizontal (black) and vertical (blue) directions, as well as their average (red). Insert: The same FTT spectrum up to 40 Hz. (B) Determination of the critical frequency via the DRIM method of one typical *S. cerevisiae* BY4742 cell in PBS after 3 h ($f_{crit} = 2.54$ Hz). (C) Histograms of f_{crit} for untreated caspofungin resistant *C. albicans* DSY4614, hypersusceptible *C. albicans* DSY1024 and wild-type *C. albicans* DSY294. (D) Histograms of f_{crit} for caspofungin treated (10 µg/ml) resistant *C. albicans* DSY4614, hypersusceptible *C. albicans* DSY1024 and wild-type *C. albicans* DSY294. The results are pooled from 1-5-hour treatments.

A



B



C

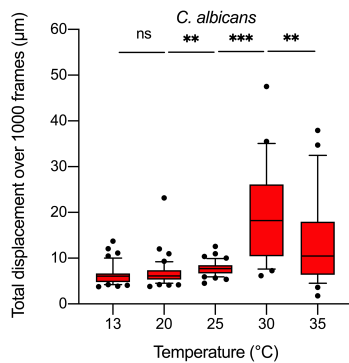


Fig. S9. Effect of the temperature and nutritional environment on the optical nanomotion of yeast cells. (A) Deep learning cells detection method. Cells automatically detected with high confidence (in green) when processing different videos. Although a few cells are missed, most of them are properly detected with high confidence. Green denotes high confidence cell, yellow denotes in threshold confidence, red indicates that detection is most likely to be an artefact. Effect of the temperature on the total displacement: results obtained with the automated detection method. Number of cells detected: (B) 147 cells (average 29 cells per condition) were analysed for *S. cerevisiae*, and (C) 194 cells (on average 39 cells per condition) were analysed for *C. albicans*. Wilcoxon test: **** P < 0.0001, *** P < 0.001, ** P < 0.01, ns: not significant.

Table S1. Yeast strains used in this study.

Micro-organism	Type	Strains	Characteristics	Genotype/Description	Reference
<i>Candida albicans</i>	Lab strain	CAF2-1	Wild type strain	$\Delta ura3::imm434/URA3$	(35)
<i>Candida albicans</i>	Lab strain	DSY1024	Mutant for efflux systems	$\Delta cdr1::hisG/\Delta cdr1::hisG; \Delta cdr2::hisG; \Delta flu1::hisG/\Delta flu1::hisG; \Delta mdr1::hisG-URA3-hisG/\Delta mdr1::hisG$	(36)
<i>Candida albicans</i>	Clinical strain	DSY294	Azole-susceptible strain	Wild type	(37)
<i>Candida albicans</i>	Clinical strain	DSY4614	Candin-resistant strain	FSK1 mutant P649H	Unpublished
<i>Candida glabrata</i>	Clinical strain	DSY562	Azole-susceptible strain	Wild type	(20)
<i>Candida lusitaniae</i>	Clinical strain	DSY4606	Wild type strain	Wild type	Unpublished
<i>Saccharomyces cerevisiae</i>	Lab strain	BY4742	Wild type strain	$MAT\alpha \ his3\Delta1 \ leu2\Delta10 \ lys2\Delta10 \ ura3\Delta10$	(38)

Movie S1. (“*S. cerevisiae*_before ethanol.m4v”)

Examples of recorded videos of yeast nanomotions: effect of ethanol on *S. cerevisiae*: *S. cerevisiae* before ethanol (70% v/v) treatment.

Movie S2. (“*S. cerevisiae*-after ethanol-60 min.m4v”)

Examples of recorded videos of yeast nanomotions: effect of ethanol on *S. cerevisiae*: *S. cerevisiae* after (60 min) ethanol (70% v/v) treatment.

Movie S3. (“video_ai-cells-detection_Candida albicans dsy294-20C.mp4”)

Examples of detection of cells using the deep learning algorithm: *C. albicans* (at a temperature of 20°C).

Movie S4. (“video_ai-cells-detection_Saccharomyces cerevisiae-30C.mp4”)

Examples of detection of cells using the deep learning algorithm: *S. cerevisiae* (at a temperature of 30°C).

REFERENCES AND NOTES

1. G. Longo, L. Alonso-Sarduy, L. Marques Rio, A. Bizzini, A. Trampuz, J. Notz, G. Dietler, S. Kasas, Rapid detection of bacterial resistance to antibiotics using AFM cantilevers as nanomechanical sensors. *Nat. Nanotechnol.* **8**, 522–526 (2013).
2. S. Kasas, F. S. Ruggeri, C. Benadiba, C. Maillard, P. Stupar, H. Tournu, G. Dietler, G. Longo, Detecting nanoscale vibrations as signature of life. *Proc. Natl. Acad. Sci. U.S.A.* **112**, 378–381 (2015).
3. K. Syal, R. Iriya, Y. Yang, H. Yu, S. Wang, S. E. Haydel, H.-Y. Chen, N. Tao, Antimicrobial susceptibility test with plasmonic imaging and tracking of single bacterial motions on nanometer scale. *ACS Nano* **10**, 845–852 (2016).
4. K. Syal, S. Shen, Y. Yang, S. Wang, S. E. Haydel, N. Tao, Rapid antibiotic susceptibility testing of uropathogenic *E. coli* by tracking submicron scale motion of single bacterial cells. *ACS Sens.* **2**, 1231–1239 (2017).
5. W. L. Johnson, D. C. France, N. S. Rentz, W. T. Cordell, F. L. Walls, Sensing bacterial vibrations and early response to antibiotics with phase noise of a resonant crystal. *Sci. Rep.* **7**, 12138 (2017).
6. C. R. Bermingham, I. Murillo, A. D. J. Payot, K. C. Balram, M. B. Kloucek, S. Hanna, N. M. Redmond, H. Baxter, R. Oulton, M. B. Avison, M. Antognozzi, Imaging of sub-cellular fluctuations provides a rapid way to observe bacterial viability and response to antibiotics. *bioRxiv* 460139 (2018).
7. M. Guizar-Sicairos, S. T. Thurman, J. R. Fienup, Efficient subpixel image registration algorithms. *Opt. Lett.* **33**, 156–158 (2008).
8. J.-S. Lee, E.-H. Park, J.-W. Kim, S.-H. Yeo, M.-D. Kim, Growth and fermentation characteristics of *Saccharomyces cerevisiae* NK28 isolated from kiwi fruit. *J. Microbiol. Biotechnol.* **23**, 1253–1259 (2013).

9. M. Lemos-Carolino, A. Madeira-Lopes, N. Van Uden, The temperature profile of the pathogenic yeast *Candida albicans*. *Z. Allg. Mikrobiol.* **22**, 705–709 (1982).
10. D. Sanglard, Emerging threats in antifungal-resistant fungal pathogens. *Front. Med.* **3**, 11 (2016).
11. M. L. Zeuthen, N. Dabrowa, C. M. Aniebo, D. H. Howard, Ethanol tolerance and the induction of stress proteins by ethanol in *Candida albicans*. *J. Gen. Microbiol.* **134**, 1375–1384 (1988).
12. A. K. Pandey, M. Kumar, S. Kumari, P. Kumari, F. Yusuf, S. Jakeer, S. Naz, P. Chandna, I. Bhatnagar, N. A. Gaur, Evaluation of divergent yeast genera for fermentation-associated stresses and identification of a robust sugarcane distillery waste isolate *Saccharomyces cerevisiae* NGY10 for lignocellulosic ethanol production in SHF and SSF. *Biotechnol. Biofuels* **12**, 40 (2019).
13. M. Schiavone, C. Formosa-Dague, C. Elsztein, M.-A. Teste, H. Martin-Yken, M. A. De Morais Jr., E. Dague, J. M. François, Evidence for a role for the plasma membrane in the nanomechanical properties of the cell wall as revealed by an atomic force microscopy study of the response of *Saccharomyces cerevisiae* to ethanol stress. *Appl. Environ. Microbiol.* **82**, 4789–4801 (2016).
14. D. Stanley, A. Bandara, S. Fraser, P. J. Chambers, G. A. Stanley, The ethanol stress response and ethanol tolerance of *Saccharomyces cerevisiae*. *J. Appl. Microbiol.* **109**, 13–24 (2010).
15. C. M. Henderson, D. E. Block, Examining the role of membrane lipid composition in determining the ethanol tolerance of *Saccharomyces cerevisiae*. *Appl. Environ. Microbiol.* **80**, 2966–2972 (2014).
16. R. G. Willaert, Micro- and nanoscale approaches in antifungal drug discovery. *Fermentation* **4**, 43 (2018).
17. D. Sanglard, F. Ischer, O. Marchetti, J. Entenza, J. Bille, Calcineurin A of *Candida albicans*: Involvement in antifungal tolerance, cell morphogenesis and virulence. *Mol. Microbiol.* **48**, 959–976 (2003).
18. N. P. Wiederhold, J. L. Grabinski, G. Garcia-Effron, D. S. Perlin, S. A. Lee, Pyrosequencing to detect mutations in *FKS1* that confer reduced echinocandin susceptibility in *Candida albicans*. *Antimicrob. Agents Chemother.* **52**, 4145–4148 (2008).

19. R. A. Cordeiro, C. E. C. Teixeira, R. S. N. Brilhante, D. S. C. M. Castelo-Branco, M. A. N. Paiva, J. J. Giffoni Leite, D. T. Lima, A. J. Monteiro, J. J. C. Sidrim, M. F. G. Rocha, Minimum inhibitory concentrations of amphotericin B, azoles and caspofungin against *Candida* species are reduced by farnesol. *Med. Mycol.* **51**, 53–59 (2013).
20. D. Sanglard, F. Ischer, D. Calabrese, P. A. Majcherczyk, J. Bille, The ATP binding cassette transporter gene *CgCDR1* from *Candida glabrata* is involved in the resistance of clinical isolates to azole antifungal agents. *Antimicrob. Agents Chemother.* **43**, 2753–2765 (1999).
21. L. Vale-Silva, E. Beaudoin, V. D. T. Tran, D. Sanglard, Comparative genomics of two sequential *Candida glabrata* clinical isolates. *G3* **7**, 2413–2426 (2017).
22. L. Castrejón, K. Kundu, R. Urtasun, S. Fidler, Annotating object instances with a Polygon-RNN, IEEE Conference on Computer Vision and Pattern Recognition (CVPR) 4485–4493 (2017).
23. O. Russakovsky, J. Deng, H. Su, J. Krause, S. Satheesh, S. Ma, Z. Huang, A. Karpathy, A. Khosla, M. Bernstein, A. C. Berg, L. Fei-Fei, ImageNet large scale visual recognition challenge. *Int. J. Comput. Vis.* **115**, 211–252 (2015).
24. J. Redmon, S. Divvala, R. Girshick, A. Farhadi, You only look once: Unified, real-time object detection, IEEE Conference on Computer Vision and Pattern Recognition (CVPR) 779–788 (2016).
25. O. Ronneberger, P. Fischer, T. Brox, in *Lecture Notes in Computer Science* (Springer Verlag, 2015), vol. 9351, pp. 234–241.
26. J. Brajtburg, W. G. Powderly, G. S. Kobayashi, G. Medoff, Amphotericin B: Current understanding of mechanisms of action. *Antimicrob. Agents Chemother.* **34** 183–188 (1990).
27. M. I. Villalba, P. Stupar, W. Chomicki, M. Bertacchi, G. Dietler, L. Arnal, M. E. Vela, O. Yantorno, S. Kasas, Nanomotion detection method for testing antibiotic resistance and susceptibility of slow-growing bacteria. *Small* **14**, 1702671 (2018).
28. A. E. Pelling, S. Sehati, E. B. Gralla, J. S. Valentine, J. K. Gimzewski, Local nanomechanical motion of the cell wall of *Saccharomyces cerevisiae*. *Science* **305**, 1147–1150 (2004).

29. B. Farzi, C. Cetinkaya, Micromechanical and surface adhesive properties of single *Saccharomyces cerevisiae* cells. *J. Phys. D Appl. Phys.* **50**, 375401 (2017).
30. A. C. Kohler, L. Venturelli, G. Longo, G. Dietler, S. Kasas, Nanomotion detection based on atomic force microscopy cantilevers. *Cell Surf.* **5**, 100021 (2019).
31. L. Alonso-Sarduy, P. De Los Rios, F. Benedetti, D. Vobornik, G. Dietler, S. Kasas, G. Longo, Real-time monitoring of protein conformational changes using a nano-mechanical sensor. *PLOS One* **9**, e103674 (2014).
32. S. van der Walt, J. L. Schönberger, J. Nunez-Iglesias, F. Boulogne, J. D. Warner, N. Yager, E. Gouillart, T. Yu; scikit-image contributors, Scikit-image: Image processing in python. *PeerJ* **2**, e453 (2014).
33. M. Alioscha-Perez, R. Willaert, H. Tournu, P. Van Dijck, H. Sahli, in *Lecture Notes in Computer Science* (Springer, Berlin, Heidelberg, 2013), vol. 8259, pp. 25–32.
34. A. Trujillo-Pino, K. Krissian, M. Alemán-Flores, D. Santana-Cedrés, Accurate subpixel edge location based on partial area effect. *Image Vis. Comput.* **31**, 72–90 (2013).
35. W. A. Fonzi, M. Y. Irwin, Isogenic strain construction and gene mapping in *Candida albicans*. *Genetics* **134**, 717–728 (1993).
36. O. Marchetti, P. A. Majcherczyk, M. P. Glauser, J. Bille, P. Moreillon, D. Sanglard, Sensitive bioassay for determination of fluconazole concentrations in plasma using a *Candida albicans* mutant hypersusceptible to azoles. *Antimicrob. Agents Chemother.* **45**, 696–700 (2001).
37. A. T. Coste, M. Karababa, F. Ischer, J. Bille, D. Sanglard, *TAC1*, transcriptional activator of *CDR* genes, is a new transcription factor involved in the regulation of *Candida albicans* ABC transporters *CDR1* and *CDR2*. *Eukaryot. Cell* **3**, 1639–1652 (2004).
38. C. B. Brachmann, A. Davies, G. J. Cost, E. Caputo, J. Li, P. Hieter, J. D. Boeke, Designer deletion strains derived from *Saccharomyces cerevisiae* S288C: A useful set of strains and plasmids for PCR-mediated gene disruption and other applications. *Yeast* **14**, 115–132 (1998).